

**OPTIMAL RHEOLOGICAL CHARACTERISTICS IN DYNAMIC STABILITY
OF POLYMER FLOW THROUGH POROUS MEDIA**

Topical Report

**By
H. W. Gao
T. R. French**

April 1988

Work Performed Under Cooperative Agreement No. FC22-83FE60149

**Prepared for
U.S. Department of Energy
Assistant Secretary for Fossil Energy**

**Jerry F. Casteel, Project Manager
Bartlesville Project Office
P.O. Box 1398
Bartlesville, OK 74005**

**Prepared by
IIT Research Institute
National Institute for Petroleum and Energy Research
P.O. Box 2128
Bartlesville, OK 74005**

TABLE OF CONTENTS

	<u>Page</u>
Abstract.....	1
Introduction.....	1
Theoretical Considerations.....	2
Adsorption/Retention.....	3
Inaccessible Pore Volume (IPV).....	3
Dispersion.....	4
Viscous Fingering.....	4
Experimental.....	4
Materials.....	4
Polymer Solution Preparation.....	5
Procedures.....	6
Results and Discussion.....	12
Flow Resistance in 10-in. Core.....	12
Displacement Tests.....	13
Frontal Analysis.....	16
Effect of Mobility Ratio.....	17
Effect of Flow Rate.....	18
Viscous Fingering.....	20
Effect of Mobility Ratio.....	21
Effect of Flow Rate.....	21
Conclusions.....	22
References.....	23

ILLUSTRATIONS

1. Schematic diagram of flow resistance apparatus.....	7
2. Calibration plot for Pusher 500 [®] constructed using the starch-triiodide method.....	10
3. Fluorescein in 1,500 ppm Pusher 500 [®]	11
4. Bromocresol green in 1,500 ppm Pusher 500 [®]	11
5. Flow behavior of Pusher 500 [®] and glycerin solutions in Berea sandstone core.....	12
6. Rheograms of Pusher 500 [®] in 53 meq/l NaCl.....	14
7. Normalized effluent concentration profiles and viscosity profile for Run 1.....	15
8. Normalized effluent concentration profiles and viscosity profile for Run 2.....	15
9. Normalized effluent concentration profiles and viscosity profile for Run 3.....	16
10. Arithmetic probability plot for tracer BCG in Runs 1, 2 and 3.....	17
11. Arithmetic probability plot for Pusher 500 [®] in Run 2.....	18
12. Normalized effluent concentration profiles and viscosity profile for Run 4.....	19
13. Normalized effluent concentration profiles and viscosity profile for Run 5.....	19

TABLE

1. Characteristics of fluids used in displacement tests at 22.4 ±0.2° C.....	5
--	---

OPTIMAL RHEOLOGICAL CHARACTERISTICS IN DYNAMIC STABILITY OF POLYMER FLOW THROUGH POROUS MEDIA

by H. W. Gao and T. R. French

ABSTRACT

To identify the optimal rheological characteristics for maintaining the dynamic stability of polymer solutions flowing through porous media, displacement tests with a Newtonian fluid and a non-Newtonian fluid were performed in a 4-ft Berea sandstone core. A solution of 63 wt pct glycerin in 53 meq/l NaCl and a solution of 1,500 ppm Pusher 500® in 53 meq/l NaCl were used as the Newtonian fluid and non-Newtonian fluid, respectively. Two flow rates, one in the purely viscous regime and one in the viscoelastic flow regime of Pusher 500 in Berea sandstone, were used in the displacement tests. The effluents collected were analyzed to determine polymer and tracer concentrations. The viscosities of the effluents were also measured with a Contraves viscometer.

By comparing the concentration profiles obtained in tests with Pusher 500 and in those with glycerin, the effects of flow rate, mobility ratio, and rheological characteristics on the dynamic stability of polymer flow in porous media were determined. At both leading and trailing edges of the polymer slug, stability increases with decreasing mobility ratio. At both high and low flow rates, a Newtonian fluid gives a more stable displacement at the fluid front than does a non-Newtonian fluid. Measurements on the mixing lengths at the back edge show that the size of the mobility buffer bank required for a flow rate at reservoir conditions (viscous flow regime) would be less for a Newtonian fluid than for a non-Newtonian fluid. At a flow rate in the viscoelastic flow regime, the required size of the mobility buffer bank is less for a non-Newtonian fluid than for a Newtonian fluid.

INTRODUCTION

In surfactant-polymer or alkaline-polymer flooding, the polymer is injected as a mobility buffer to preserve the integrity of the chemical slug and to improve the sweep efficiency. When designing a polymer bank for these floods, both mobility ratio and slug size of polymer bank have to be considered. The required mobility ratio has to account for polymer loss from

shear, thermal, chemical, or bacterial degradation. The required slug size must also take into account polymer adsorption/retention, mixing, and inaccessible pore volume (IPV) so that a favorable mobility ratio between the chemical and polymer slugs can be maintained as they travel from the injection wells to the producing wells.

Many displacement tests have been performed to investigate these phenomena.¹⁻⁸ Vossoughi, et al.⁹ developed a model to simulate miscible displacement by polymer solutions, including the effects of retention, IPV, dispersion, and viscous fingering. Lecourtier and Chauveteau⁵ proposed a theoretical model taking into account the pore wall exclusion mechanism to predict the rod-like polymer velocity in porous media and the spreading out of polydispersed polymer slugs. Sorbie, et al.⁷ conducted an experimental and theoretical study of polymer flow in porous media. The phenomena they studied included polymer-tracer dispersion, excluded-inaccessible volume effects, adsorption, and viscous fingering. None of these studies considered the roles of different rheological characteristics in maintaining the dynamic stability of polymer slugs flowing through porous media.

This research was concerned with the polymer rheological characteristics that are optimal for the displacement of a fluid by a polymer solution in porous media. Displacement tests with a Newtonian fluid and a non-Newtonian fluid in a 4-ft core were performed in the absence of adsorption. Two flow rates, one in the purely viscous flow regime and one in the viscoelastic flow regime of the non-Newtonian fluid, as determined in a 10-in. Berea sandstone core, were used. At these two flow rates, both Newtonian and non-Newtonian fluids gave the same magnitudes of resistance factor. Effluent concentration profiles were used to illustrate the effects of different rheological characteristics, mobility ratio, and flow rate on the dynamic stability of polymer slugs flowing through porous media.

THEORETICAL CONSIDERATIONS

In chemical (micellar-polymer or alkaline-polymer) flooding, two transition zones exist at both leading and trailing edges of the polymer slug. In these zones, the shape of the polymer slug as indicated by the concentration profile is altered. The factors that cause alteration of the polymer concentration profile are adsorption/retention, inaccessible pore

volume (IPV), and dispersion at the front edge and IPV, dispersion, and viscous fingering at the back edge.

Adsorption/Retention

Adsorption/retention tend to denude the polymer front and spread out the polymer concentration profile at the leading edge. Adsorption is the retention of polymer molecules on a surface by electrostatic forces. The amount of polymer adsorbed on the rock surface strongly depends on the type and size of polymer molecules, polymer concentration, rock surface properties, solution environment, and temperature.¹⁰⁻²²

Mechanical entrapment of polymer molecules in porous media during polymer flow is caused by the large size of polymer molecules relative to the size of the pore openings,^{10,23} or by an ultrafiltration phenomenon.²⁴

In addition to adsorption and mechanical entrapment, polymer can also be retained in the porous media under the influence of hydrodynamic forces. Several investigators have found that the amount of polymer retained during polymer flow increases with increasing flow rate²⁵⁻²⁷ or with decreasing mobility.²⁶ As the flow rate was decreased to that of the original, the same extra polymer that was retained when the flow rate was increased was expelled; hence, this process is somewhat reversible and has been referred to as hydrodynamic retention.²⁸

Inaccessible Pore Volume (IPV)

In the absence of adsorption, polymer molecules propagate through reservoir rock at a faster rate than small molecules such as water or an ethanol tracer.^{1,28} This is attributed to a phenomenon called inaccessible pore volume (IPV). Inaccessible pore volume is that part of the pore volume that is not contacted by flowing polymer molecules.

Several mechanisms that have been proposed to explain the cause of IPV are (1) the large molecules being excluded from small pores,²⁸ (2) hydrodynamic exclusion,^{1,29} and (3) the volume occupied by the retained polymer molecules on the rock surfaces.²⁸ Because of IPV, polymer can invade and dilute the chemical slug ahead. This will affect the mobility and stability of the chemical slug and the required volume of mobility buffer bank.

Dispersion

Dispersion is the additional mixing beyond that due to molecular diffusion during the displacement of one fluid by another miscible fluid.³⁰ Dispersion increases with flow rate, inhomogeneity of porous media, and the viscosity ratio between the displaced and displacing fluids.³⁰⁻³¹ At high flow rates, mixing theories predict that K is proportional to u or u^2 ,³¹ where K is the dispersion coefficient and u is the interstitial velocity. Experimental exponent values ranging from 1.0 to 1.2 have been reported.^{7,31} Dispersion increases the spreading out of concentration profiles at both edges. In the absence of adsorption and IPV effect, the spreading out of the concentration profiles at the polymer front, where the mobility ratio is favorable and the displacement is stable, is mainly caused by dispersion.³²

Viscous Fingering

At the trailing edge, the more viscous polymer is displaced by a less viscous brine; hence, the mobility ratio is unfavorable and the displacement is unstable. Because of unstable displacement, viscous fingering occurs. Fingers are initiated by permeability variations.³³ The growth and propagation of fingers are affected by both mobility ratio and permeability distribution. In the absence of IPV, viscous fingering has been proven to be the dominant mechanism that causes the spreading out of the concentration profiles.^{9,32}

EXPERIMENTAL

Materials

The 10-in. long by 1.5-in. diameter and 4-ft long by 2-in. diameter cylindrical Berea sandstone cores used in this study were cut along the bedding plane of two blocks of sandstone from Cleveland Quarries in Ohio and fired at 485° C for 24 hr. The 10-in. core has a porosity of 21 pct and a brine permeability of (576 ± 7 md). The 4-ft core has a porosity of 20.7 pct and a brine permeability of (574 ± 6 md).

A 63-wt pct glycerin solution in 53 meq/l NaCl and a solution of 1,500 ppm Pusher 500 in 53 meq/l NaCl were used as the Newtonian and non-

Newtonian fluids in displacement tests, respectively. The injection of each fluid was preceded and followed by a thickened brine (53 meq/l NaCl). Table 1 lists the sequence of fluids injected through the core. In test 1, the brine was thickened with 46.5 wt pct sucrose. In tests 2 through 5, the brine was thickened with 56 wt pct glycerin. A bactericide, 0.1 percent by volume of 37.37 percent formaldehyde solution, was used in all solutions. In displacement tests, two tracers, 800 ppb fluorescein (FC) and 2,400 ppb bromocresol green (BCG), were used to label the thickened brine and the middle slug, respectively. The viscosities of 63 wt pct glycerin solution in 53 meq/l NaCl, the brine thickened with 56 wt pct glycerin and the brine thickened with 46.5 wt pct sucrose at 22.4° C are 12.66, 8.13, and 10.8 cp, respectively. All solutions were filtered through a 115-mesh stainless steel screen before viscosity measurements and injection through cores.

Polymer Solution Preparation

The polymer used was Dow Pusher 500[®], a partially-hydrolyzed polyacrylamide in powder form, having a weight average molecular weight of 4.5 million and supplied by Dow Chemical Company. Its rheological behavior has been extensively studied in our laboratory.³⁴⁻³⁵ Throughout this study, a polymer concentration of 1,500 ppm in 53 meq/l NaCl diluted from a 7,500 ppm stock solution was used, and 0.1 percent by volume of 37.37 percent

TABLE 1. - Characteristics of fluids used in displacement tests at 22.4 ± 0.2° C

Run number	Injection sequence	Flow rate, ft/day	Mobility ratio at		Size of middle slug injected, PV	Size of chase brine injected, PV	Chase brine breakthrough, PV	Mixing length at back edge, ft
			front edge	back edge				
¹	Brine/Pusher 500/brine	18.1	0.85	1.17	3.42	2.65	0.86	1.06
²	Brine/Pusher 500/brine	18.1	0.64	1.56	3.32	2.26	0.86	1.14
³	Brine/glycerin/brine	18.1	0.64	1.56	3.22	2.4	0.79	2.48
⁴	Brine/glycerin/brine	1.27	0.64	1.56	2.21	1.94	0.81	1.76
⁵	Brine/Pusher 500/brine	1.27	0.64	1.56	3.27	2.16	0.68	2.08

¹Brine was thickened with 46.5 wt pct sucrose (10.8 cp) in test 1.

²Brine was thickened with 56 wt pct glycerin (8.13 cp) in tests 2 through 5.

³The viscosity of glycerin (63 wt pct) in tests 3 and 4 was 12.7 cp.

⁴Bulk solution viscosities of Pusher 500 at shear rates corresponding to 18.1 and 1.27 ft/day were 9 cp and 18.5 cp, respectively.

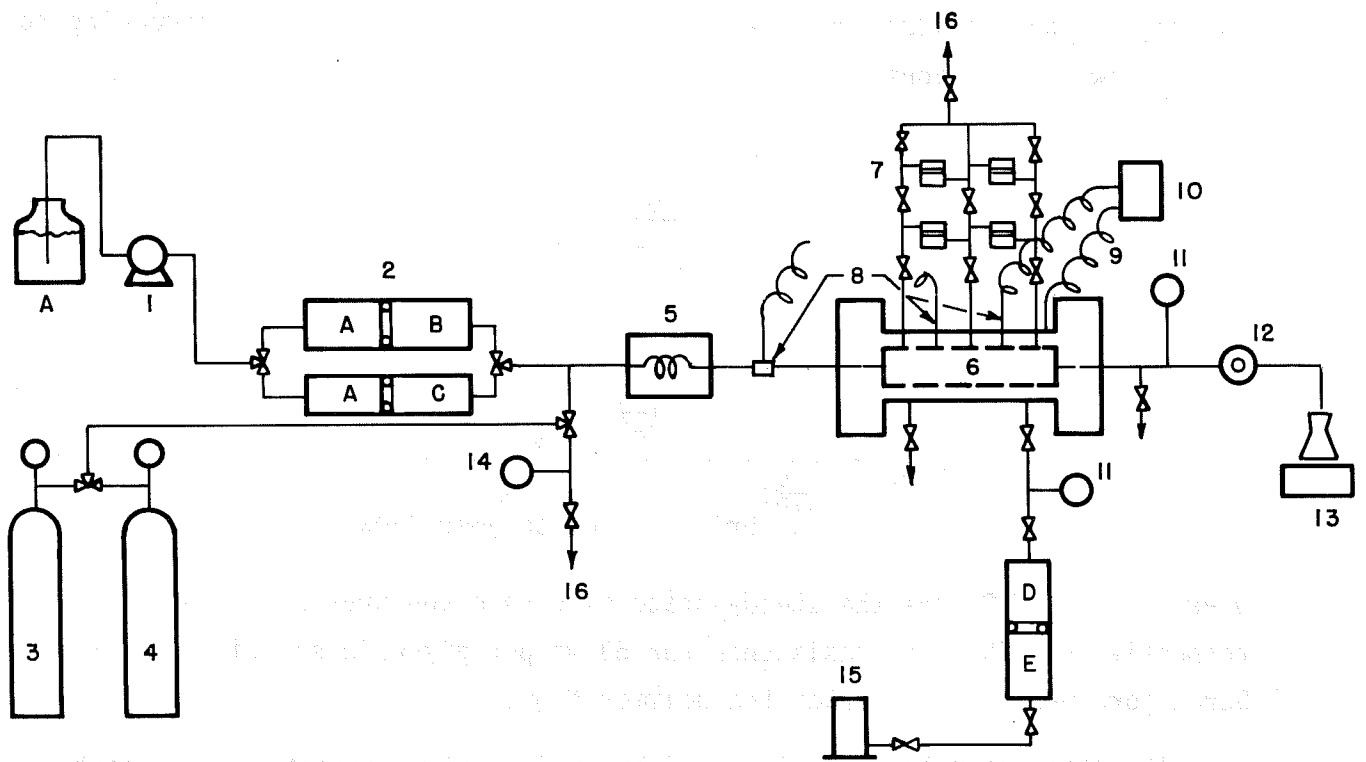
formaldehyde solution was added to the solution as a biocide. The viscosities of the polymer solution used were 18.5 cp at 8.4 sec⁻¹ and 9 cp at 129 sec⁻¹. In displacement tests, the polymer solution also contained 2,400 ppb bromocresol green (BCG) as a tracer. The solution was filtered through a 115-mesh stainless steel screen before rheological characterization and injection through cores.

The stock solution was made by sprinkling the powdered polymer into the vortex of deionized water over a period of 30 seconds while stirring with a caged stirrer and mixed for 3 hours. The solution was allowed to stand overnight before diluting to 7,500 ppm. The stock solution was then transferred into a plastic bottle and stored in a refrigerator when it was not in use. The proper dilution and salt, biocide, and tracer compositions were prepared on the day when tests were made.

Procedures

All experiments were conducted at 22.4 ± 0.2° C. Viscosity of each fluid was measured with a LS-30 Contraves viscometer. Baseline displacement tests require a complete set of flow resistance data for both Newtonian and non-Newtonian fluids. Because of the time constraint, a 10-in. core was used for flow resistance measurements. Figure 1 shows the apparatus for measuring the flow resistance of polymer and that of 63 wt pct glycerin in Berea core. A constant flow-rate pump was used to inject the fluids through the core. The two fluid isolators allow the injection of test fluids and brine without contacting the pump. The core was mounted horizontally in a Hassler sleeve with pressure taps situated 1, 5, and 9 in. from the core inlet. To avoid end effects, pressure drops were measured with Validyne pressure transducers across the first and second taps and across the second and third taps. At low flow rates (<2 ft/day), pressure drops were measured across the first and third taps.

Before injection, all fluids were degassed. After the core was evacuated and checked for leaks, it was saturated with brine. Steady-state pressure drops over the two intervals and flow rates were then measured for the brine before and after the polymer flow, and for the polymer flow. The flow rate was measured by weighing the increments of effluent with time. The resistance



- | | | | |
|-----------------------|-----------------------------|--------------------------------------|-----------------------------|
| A. Displacement fluid | 1. Constant flow-rate pump | 6. Core | 11. Pressure gauge |
| B. Brine solution | 2. Fluid isolators | 7. Pressure transducers and manifold | 12. Back pressure regulator |
| C. Test fluid | 3. Air cylinder | 8. Thermocouple | 13. Balance |
| D. D.I. Water | 4. CO ₂ cylinder | 9. Heating tape wire | 14. Vacuum gauge |
| E. Hydraulic fluid | 5. Preheater | 10. Temperature controller | 15. Hydraulic pump |
| | | | 16. To vacuum pump |

FIGURE 1. - Schematic diagram of flow resistance apparatus.

factor, F_R , and residual resistance factor, F_{Rr} , were calculated according to the following equations:³⁴

$$F_R = \frac{\left(\frac{Q}{\Delta P}\right)_{\text{brine}}}{\left(\frac{Q}{\Delta P}\right)_{\text{polymer or glycerin}}} \quad (1)$$

$$F_{Rr} = \frac{\left(\frac{Q}{\Delta P}\right)_{\text{brine}}}{\left(\frac{Q}{\Delta P}\right)_{\text{brine, after polymer flow}}} \quad (2)$$

where Q and ΔP are the steady-state flow rate and pressure drop, respectively. The flow resistance for 63 wt pct glycerin solution in the same Berea core was measured after the polymer flow.

The same apparatus was also used to perform displacement tests except that the 10-in. coreholder was replaced by a 4-ft coreholder and that a fraction collector was used to collect the effluents. The pressure drop across the core was measured with a Validyne pressure transducer calibrated from 0 to 500 psi. Throughout the tests, both fluid isolators were exposed to the same pressure. This was to avoid a change in flow rate during the switch of injection fluid. The switch of injection of one fluid to another was made through a 3-way valve.

To eliminate the adsorption problem during displacement tests, the 4-ft core was pretreated with 4 PV of 1,500 ppm Pusher 500 solution, followed by injection of 10 PV of brine (53 meq/l NaCl). After the treatment, the measured residual resistance factor on the 4-ft core ($F_{Rr} = 1.99$) at 18.2 ft/day was within 3 percent of that measured on the 10-in. core ($F_{Rr} = 1.93$).

The method developed by Scoggins and Miller³⁷ was used to determine the polymer concentrations in the effluents. This method involves the oxidation of Pusher 500 with bromine at pH 5.5 to give a product that oxidizes iodide ion to iodine. A 1M sodium acetate-acetic acid buffer solution having a pH of 5.5 was used. After destroying the excess oxidizing agent (bromine) with sodium formate, starch- CdI_2 reagent was added as both color reagent and source

of iodide ion. The absorbance of starch-triiodide at 610 nm was measured with a Bausch Lomb Spectronic 20 versus a reagent blank. The resulting calibration plot shown in figure 2 shows that Beer's law is obeyed at polymer concentrations from 0 to 300 ppm.

A Beckman Model 26 spectrophotometer was used to conduct wavelength scans and calibration curves. Absorbance by both FC and BCG was determined to be light-sensitive and pH-sensitive. The tracers were protected from light, and prior to measuring absorbance, the pH of the effluents was adjusted to 9 with a 0.6 N NaOH solution. The calibration curve for FC is shown in figure 3, and the calibration curve for BCG is shown in figure 4. FC absorbance was measured at 490 nm wavelength and BCG absorbance was measured at 615 nm. The BCG absorbance interferes at 490 nm with the FC absorbance. The FC absorbance was therefore corrected, when necessary, for the interference from BCG.

Chromatographic separation of tracers from the labeled slugs and irreversible adsorption onto the Berea sandstone cores were considered as potential problems in the tracer analyses. A test was conducted with a 10-in. Berea sandstone core that had previously been polymer flooded to determine if FC would be permanently adsorbed. The 10-in. core was first flooded with 8.9 PV of Pusher 500 polymer solution. A volume of brine labeled with 800 ppb FC equal to 1.05 PV was then injected through the core. The 1.05 PV of FC solution was followed by 1.44 PV of unlabeled brine. Since 98.41 percent of the FC was recovered, it was concluded that permanent adsorption of FC (and presumably BCG, a similar organic compound) posed no serious problem.

The results of the 4-ft core tests with glycerin were used to determine if chromatographic separation of tracers from the labeled slugs was occurring. The glycerin slug was labeled with bromocresol green (BCG). The viscosity of a 50:50 mixture of thickened brine-glycerin solution was compared to the viscosity of the fractions collected during the corefloods at 50 percent BCG tracer concentration. This composition indicated an error of 0.01 PV at the glycerin front in floods 3 and 4 (see table 1). This corresponds to an error of less than 0.1 percent PV and poses no problem in data interpretation.

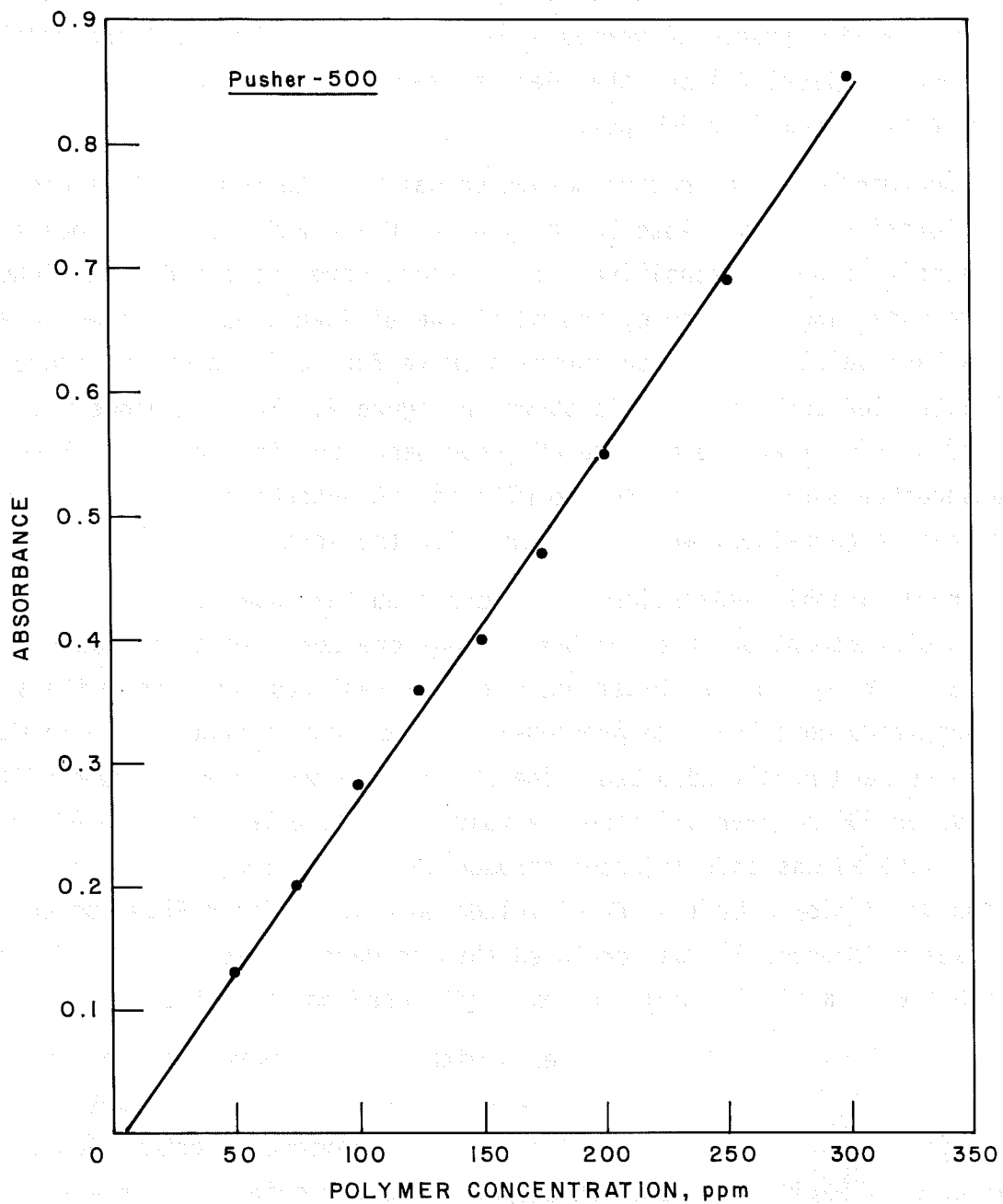


FIGURE 2. - Calibration plot for Pusher 500[®] constructed using the starch-triiodide method.

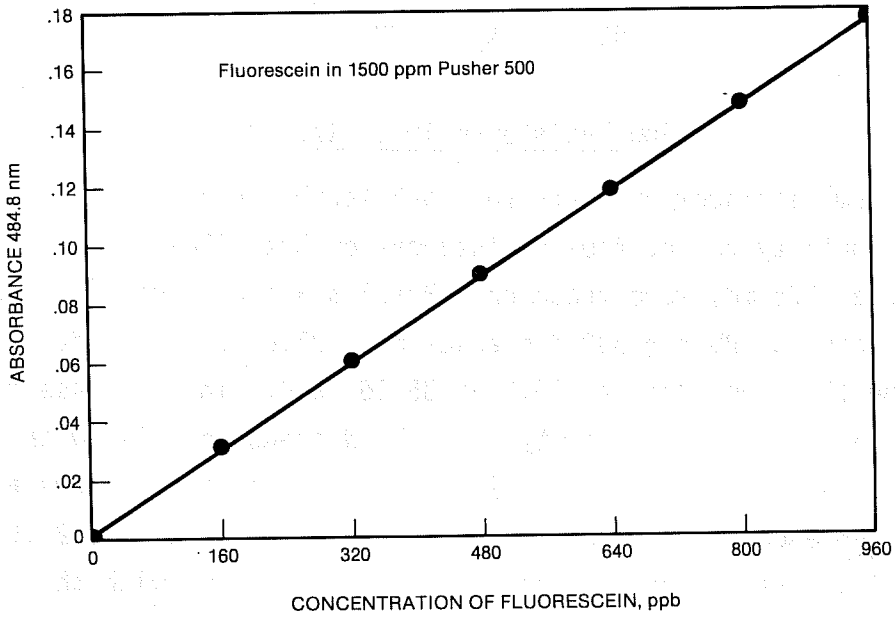


FIGURE 3. - Fluorescein in 1,500 ppm Pusher 500®.

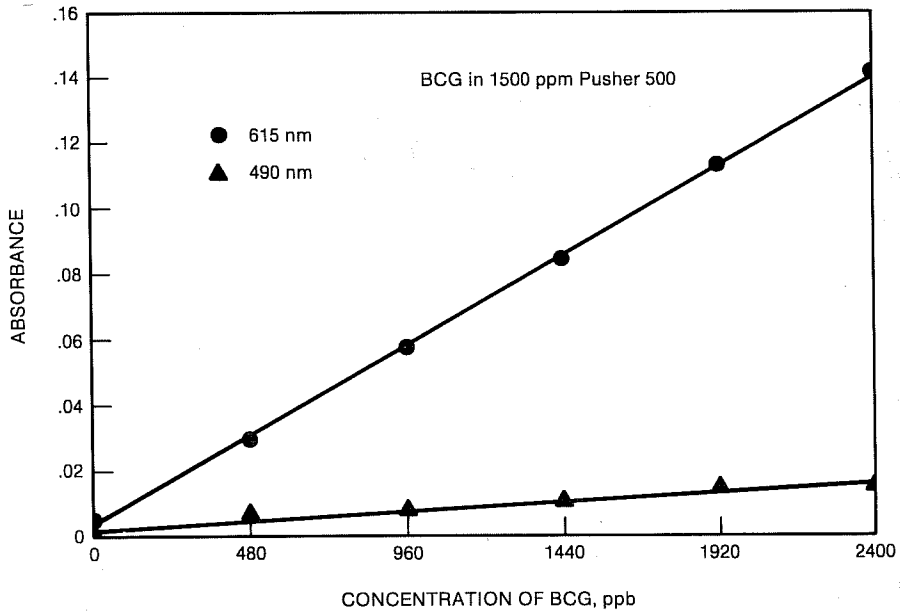


FIGURE 4. - Bromocresol green in 1,500 ppm Pusher 500®.

RESULTS AND DISCUSSION

Flow Resistance in 10-in. Core

To perform displacement tests for both Newtonian and non-Newtonian fluids at the same mobility ratio, flow resistances of both fluids in a 10-in. Berea sandstone core (576 md) were measured. Results are plotted in figure 5. The resistance factor of Pusher 500 decreases from 25.8 at 0.0295 ft/d to 16.67 at 5.56 ft/d and then increases to 30.2 at 35.26 ft/d. The increase of F_R with flow rate is due to viscoelasticity, and the decrease of F_R with flow rate is due to pseudoplasticity. The residual resistance factor shows a slight flow-rate dependence. It increases from 1.61 at 0.623 ft/d to 2.15 at 35.8 ft/d. The flow-rate dependence for F_R and F_{Rr} agrees with that previously reported.³⁴⁻³⁵ Compared with the data obtained in a 365-md Berea sandstone core,³⁴⁻³⁵ both F_R and F_{Rr} decrease with k/ϕ , where k is brine permeability, and ϕ is porosity.

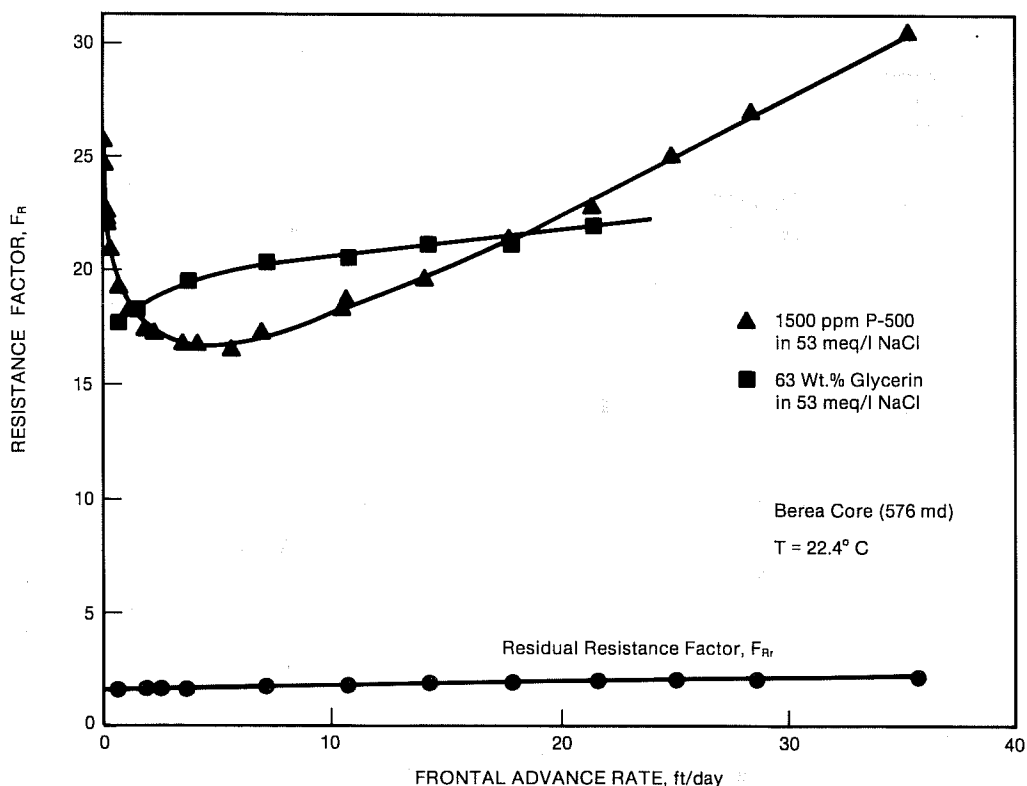


FIGURE 5. - Flow behavior of Pusher 500® and glycerin solutions in Berea sandstone core.

The resistance factor for the 63 wt pct glycerin in the same Berea sandstone core as shown in figure 5 increases from 17.7 at 0.695 ft/d to 22.06 at 21.45 ft/d. The glycerin solution is a Newtonian fluid and has a bulk solution viscosity of 12.66 cp at 22.4° C. One of the factors that cause the flow-rate dependence of F_R for the glycerin solution in Berea sandstone core is the residual resistance factor. At flow rates below about 3 ft/d, F_R decreases with decreasing flow rate dramatically. The reason for this is not clear. One possible explanation is that the configuration of the adsorbed polymer changed drastically in this low flow rate regime.

At frontal advance rates of about 1.27 and 18.1 ft/d, Pusher 500 and glycerin solution in Berea sandstone core give the same magnitudes of resistance factor. The corresponding shear rates for these two flow rates are 8.36 and 129 sec^{-1} , respectively.³⁴⁻³⁵ As seen from figure 6, 8.36 sec^{-1} is in the purely viscous flow region, and 129 sec^{-1} is in the viscoelastic flow region. These two flow rates were used in later displacement tests in a 4-ft Berea sandstone core. The viscous flow process for Pusher 500 in the 576-md Berea sandstone core persists up to a shear rate of about 22.8 sec^{-1} . At this shear rate, the apparent viscosity begins to deviate from the power law (power-law index = 0.898), indicating the onset of viscoelasticity effects. The corresponding Deborah number for this shear rate is 0.014, in agreement with previous findings.³⁴⁻³⁵

As for a 365-md Berea sandstone core,³⁴⁻³⁵ the apparent viscosity of Pusher 500 in the purely viscous flow region in the 576-md Berea sandstone core is lower than the solution viscosity. This can be attributed to a depleted-layer effect.³⁸ As seen from figure 6, this effect increases with decreasing pore size and shear rate. The same effect has also been observed by Chauveteau.²⁷⁻³⁸ Figure 6 also reveals that the minimum apparent viscosity for Pusher 500 in the 576-md Berea sandstone core occurs at a shear rate of about 37 sec^{-1} (5.56 ft/d). The equivalent Deborah number for this shear rate is 0.0232. This conforms to a previous finding that the minimum values of apparent viscosities occur at a Deborah number between 0.01 to 0.03.³⁵

Displacement Tests

Five displacement tests as shown in table 1 were performed during this study. Test 1 was performed at a favorable mobility ratio of 0.85 at the

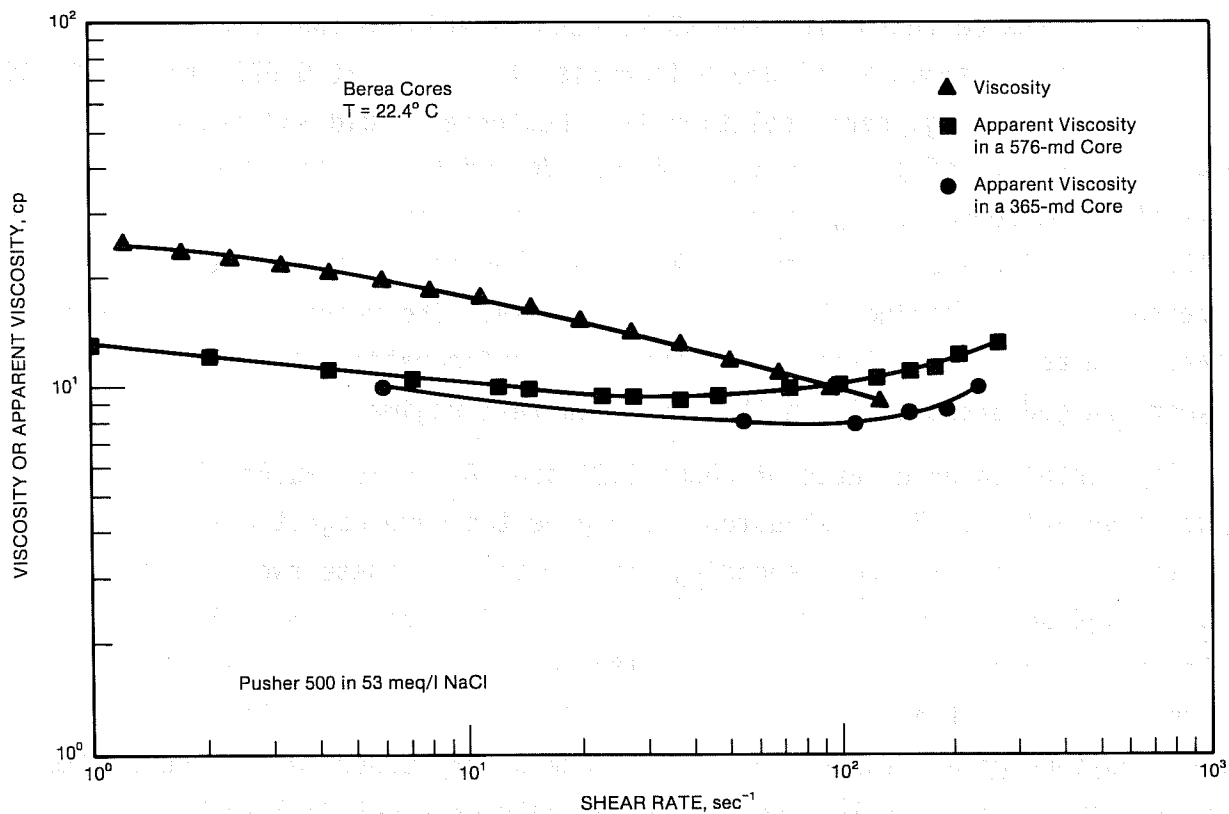


FIGURE 6. - Rheograms of Pusher 500[®] in 53 meq/l NaCl.

front edge and an unfavorable mobility ratio of 1.17 at the back edge. Tests 2 to 5 were performed at a favorable mobility ratio of 0.64 at the leading edge and an unfavorable mobility ratio of 1.56 at the trailing edge. Typical results of the effluent analyses are plotted in figures 7 through 9 for tests 1, 2, and 3, respectively. Figures 7 and 8 are for displacement tests with Pusher 500, and figure 9 is for the test with 63 wt pct glycerin. As shown in figures 7 and 8, polymer leads tracer (BCG) at both leading and trailing edges. This is due to inaccessible pore volume (IPV).¹ The area between the two concentration profiles at the back edge is a measure of IPV, and the difference between the two areas at both edges is a measure of polymer adsorption/retention. Calculated IPV and polymer adsorption/retention are 4.7 and 2.3 percent PV, respectively, in test 1 and 4.5 and 2.8 percent PV,

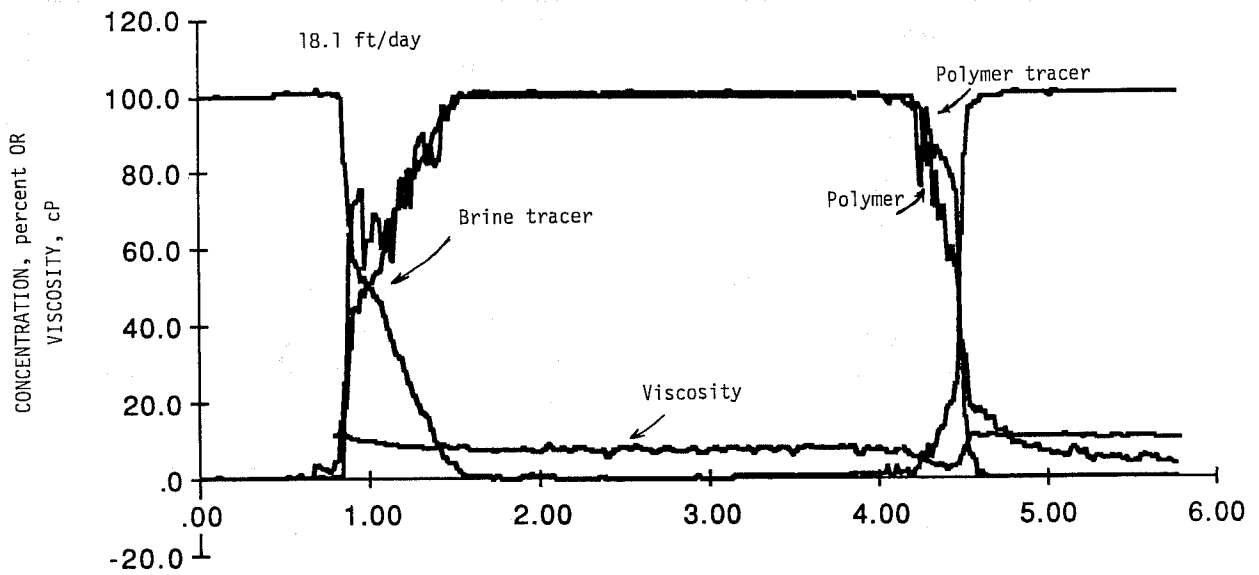


FIGURE 7. - Normalized effluent concentration profiles and viscosity profile for Run 1.

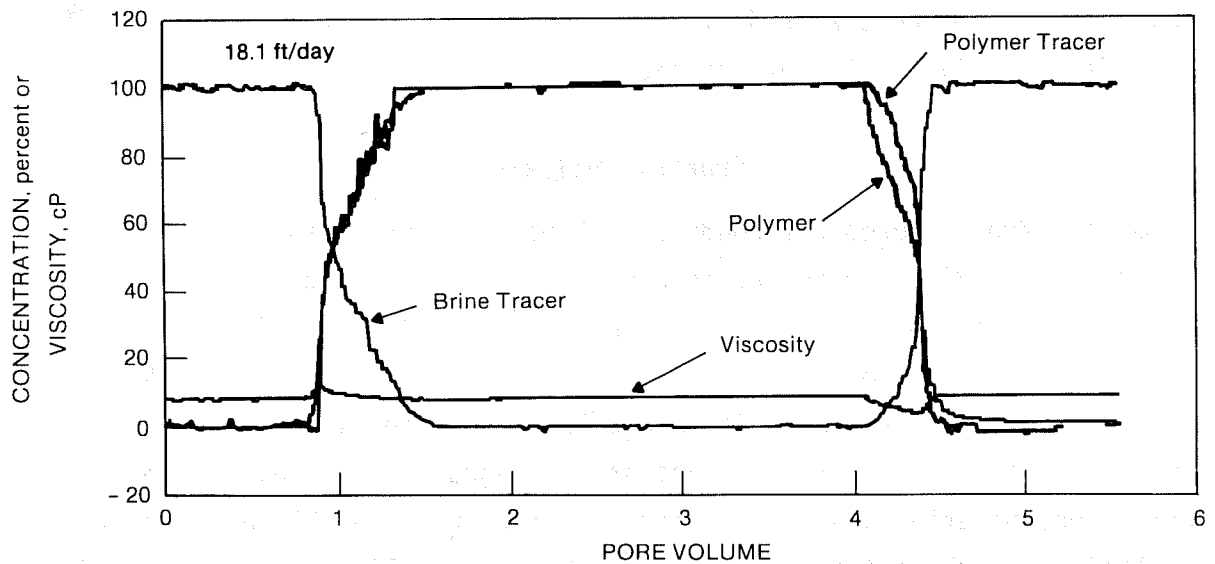


FIGURE 8. - Normalized effluent concentration profiles and viscosity profile for Run 2.

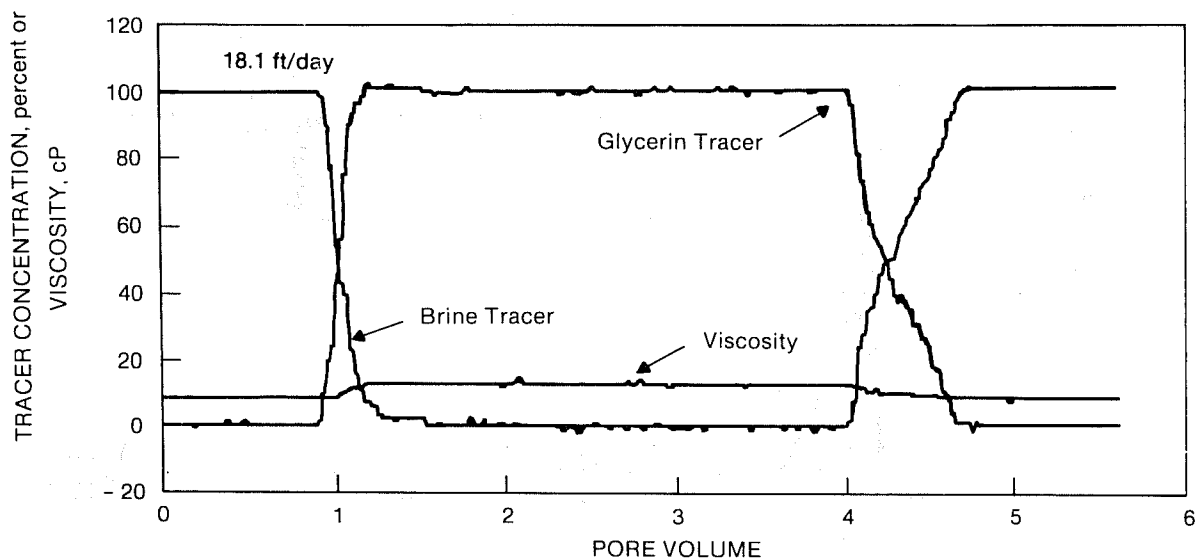


FIGURE 9. - Normalized effluent concentration profiles and viscosity profile for Run 3.

respectively, in test 2. Low polymer retention in the core is due to the pretreatment of the core with 4 PV of Pusher 500 before the displacement tests. This simplifies the explanation of the results.

Frontal Analysis

As seen from figures 7 through 9, polymer, polymer tracer (BCG), and glycerin tracer (BCG) concentration profiles are all spread out at both edges. Since there are no adsorption-retention problems and IPV effect for tracers, the spreading out of the tracer concentration profiles at the leading edge, where the mobility ratio is favorable, is due to dispersion.³² Comparison of the polymer tracer concentration profile in figure 8 and the glycerin concentration profile in figure 9 shows that the glycerin front is more stable than the polymer front. From the probability plot shown in figure 10, the longitudinal dispersion coefficients, calculated after Brigham,³¹ for BCG tracer in Pusher 500 and in glycerin at a mobility ratio of 0.64 are 2.06×10^{-2} and 1.2×10^{-3} cm^2/sec , respectively. This indicates that at the same favorable mobility ratio and flow rate, the front of a Newtonian fluid is more

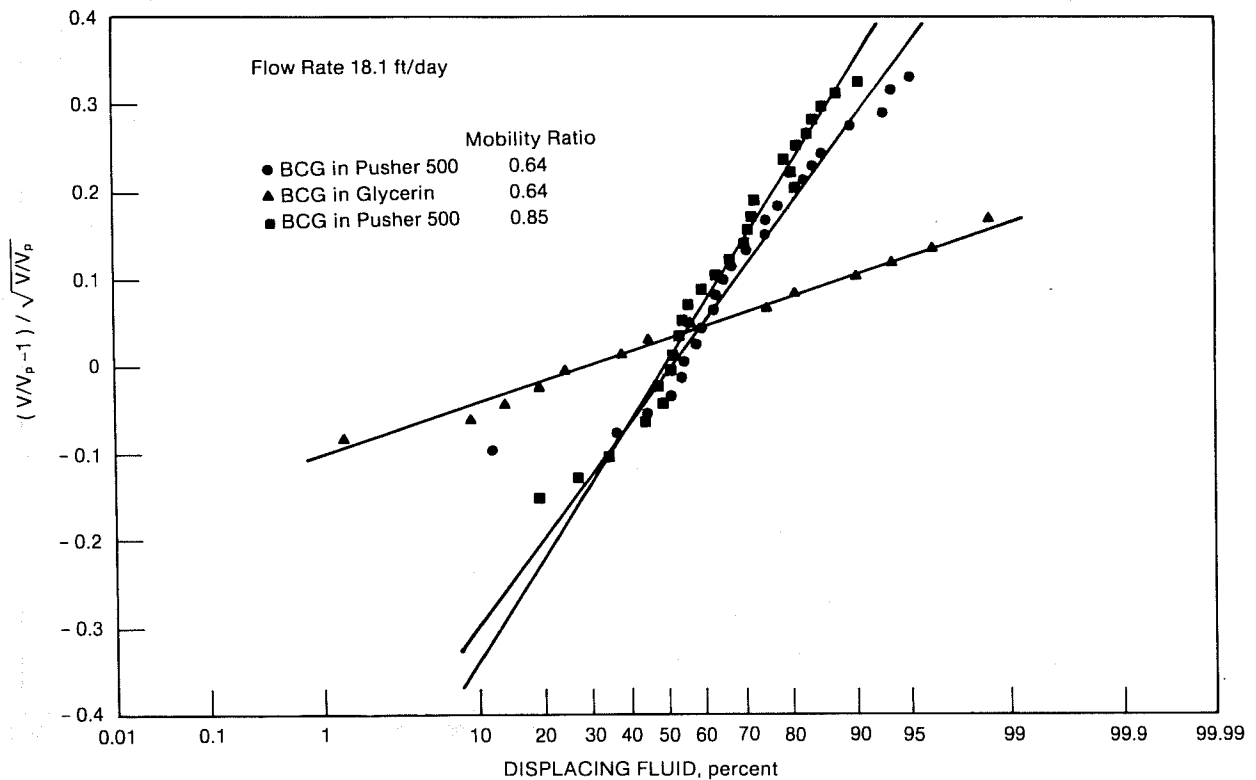


FIGURE 10. - Arithmetic probability plot for tracer BCG in Runs 1, 2 and 3.

stable than that of a non-Newtonian fluid. The calculated dispersion coefficient for polymer in test 2 (shown in figure 11) is $2.64 \times 10^{-2} \text{ cm}^2/\text{sec}$. This value is slightly higher than that of the polymer tracer. This can be attributed to IPV (4.7 percent PV) and retention (2.3 percent PV) effects although both of them are small. Sorbie, et al.⁷ also observed higher (2 to 4 times) dispersion coefficients for xanthan biopolymer than polymer tracer in a Clashach sandstone core. They attributed this to the excluded volume (about 8 percent PV) effect. In figures 10 and 11, V is the volume injected and V_p is the total pore volume.

Effect of Mobility Ratio

The calculated longitudinal dispersion coefficient for the polymer tracer in test 1 (mobility ratio = 0.85) is $2.82 \times 10^{-2} \text{ cm}^2/\text{sec}$. Compared with test 2

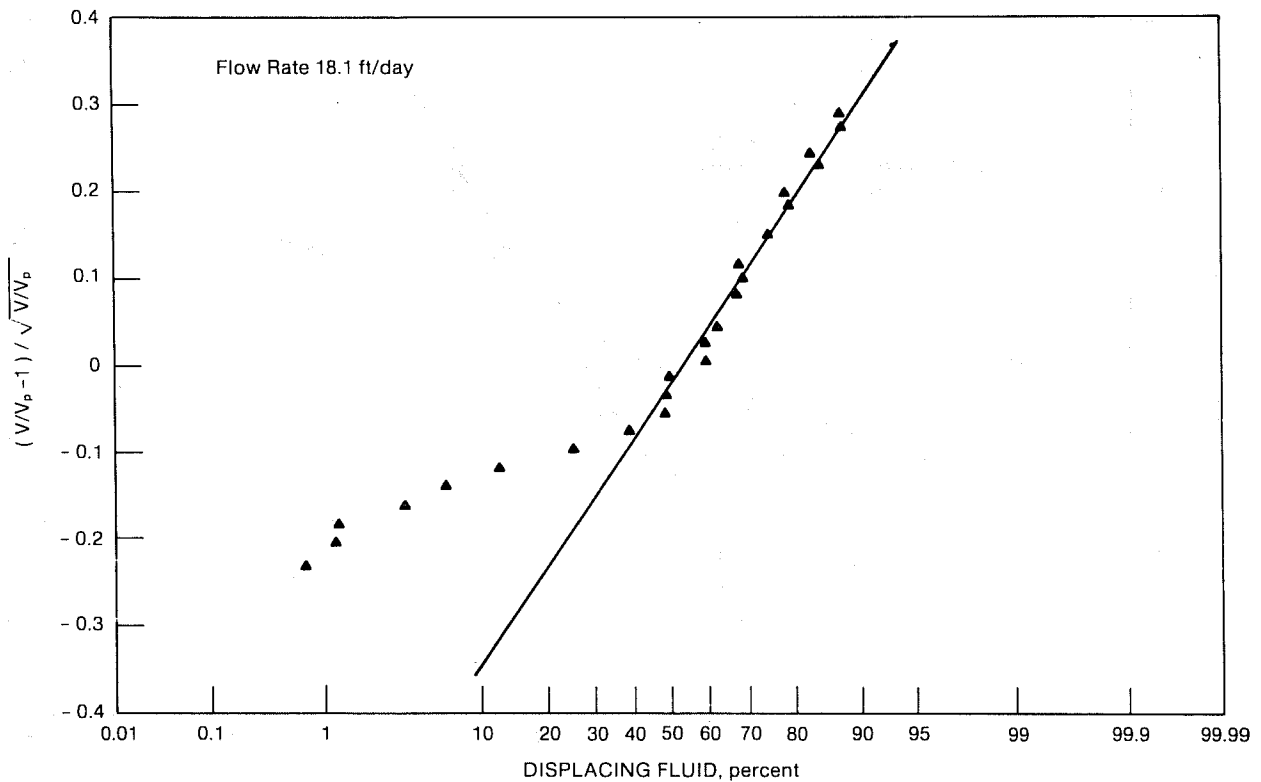


FIGURE 11. - Arithmetic probability plot for Pusher 500® in Run 2.

(mobility ratio = 0.64), the dispersion coefficient of polymer tracer in test 1 increases by a factor of 1.37. This factor is close to the ratio (1.33) between the two mobility ratios in tests 1 and 2. This finding agrees with the observation made by Brigham that both dispersion coefficient and viscosity ratio are changed by the same factor when the viscosity ratio is favorable.³¹

Effect of Flow Rate

Tests at a rate of 1.27 ft/day (figures 12 and 13) also show a more stable front for glycerin solution than for the Pusher 500. At this low flow rate, calculated dispersion coefficients for BCG tracer-in-polymer, polymer, and BCG tracer in glycerin are 4.66×10^{-4} , 5.33×10^{-4} , and 6.42×10^{-5} cm²/sec, respectively. Like the test at a high flow rate, the dispersion coefficient for polymer is higher than that of the polymer tracer. The two flow rates

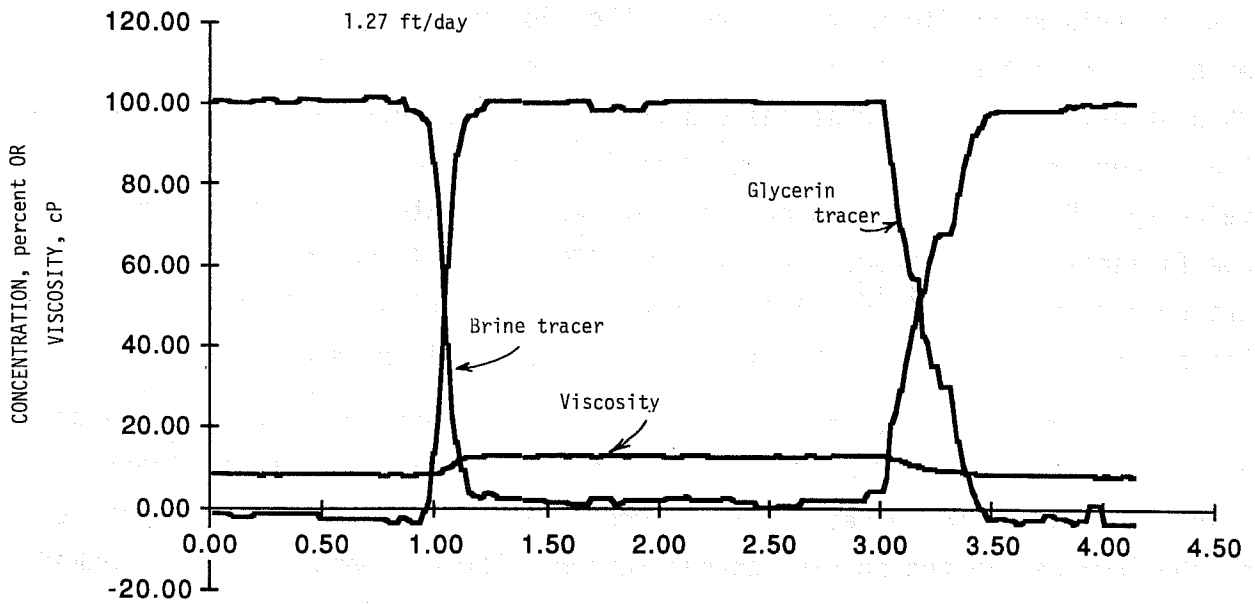


FIGURE 12. - Normalized effluent concentration profiles and viscosity profile for Run 4.

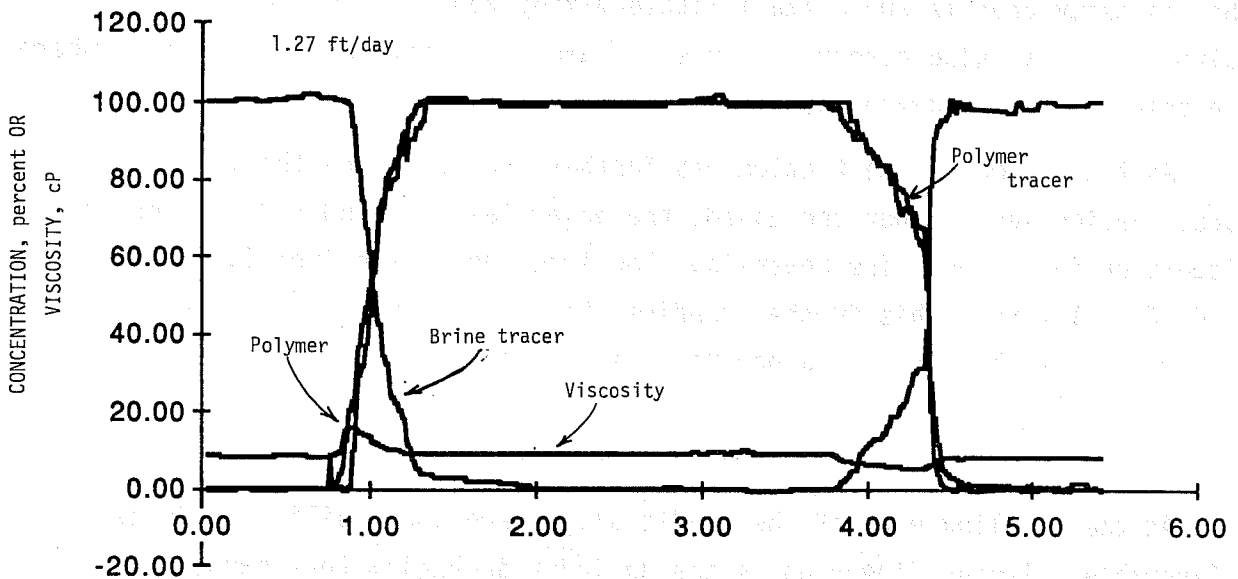


FIGURE 13. - Normalized effluent concentration profiles and viscosity profile for Run 5.

used in this study lie in the range of the flow rates used by Sorbie, et al.⁷ The permeability of the core they used is higher than that used in this study. They found that the dispersion coefficients for both polymer and tracer were all proportional to $u^{1.0}$ to 1.2 , where u is the interstitial velocity. Based on the data obtained at two flow rates, the dispersion coefficients for BCG tracer in glycerin, BCG tracer in polymer, and polymer are proportional to $u^{1.13}$, $u^{1.43}$, and $u^{1.47}$, respectively. These exponents lie between the 1.00 and 2.00 limits predicted by mixing theories.³¹

Figure 8 also shows the viscosity of the effluents measured at a shear rate of 120 sec^{-1} . At 0.81 PV where the polymer broke out, the effluent viscosity started to increase. The increase in effluent viscosity is caused by the increase in the polymer concentration. The effluent viscosity peaked at 0.89 PV and then started to decrease. The decrease in viscosity is due to the decreasing glycerin concentration. The hump in the viscosity profile corresponds to a little mixing zone between 0.87 and 0.93 PV. In this zone, the power-law-fluid flow index decreased from 0.96 at 0.87 PV to 0.85 at 0.93 PV. In this region, the dispersion coefficients for BCG tracer and polymer as determined from the lower slope values in the probability plots in figures 10 and 11 are 1.0×10^{-3} and $1.32 \times 10^{-3} \text{ cm}^2/\text{sec}$, respectively. A similar hump in the viscosity profile and a small little-mixing zone at the front of the polymer slug was also observed in tests 1 and 5 but not in tests 3 and 4 where the test fluids are glycerin.

As the polymer concentration was further increased and the glycerin concentration was further decreased, the power-law flow index decreased and dispersion increased. The power-law flow index decreased from 0.84 at 0.95 PV to 0.76 at 1.4 PV. This further confirms that the front of a Newtonian fluid is more stable than that of a non-Newtonian fluid.

Viscous Fingering

At the trailing edge of the middle slug where the mobility ratio is unfavorable, viscous fingering is the dominant mechanism that causes the spreading out of concentration profiles.³² At a flow rate of 18.1 ft/day, the tracer, fluorescein (FC), in the chase brine broke through at 0.86 PV in test 2 and 0.79 PV in test 3 after the injection of chase brine. The mixing

length, defined as the equivalent length for 5 to 95 percent concentration range for the effluents,³⁹ was 1.14 ft in test 2 and 2.48 ft in test 3, as shown in table 1. The earlier breakthrough of chase brine and the longer mixing-zone length in test 3 than in test 2 indicate that Pusher 500 in the viscoelastic flow regime gives less viscous fingering than does the glycerin. The reason for this is explained later.

Effect of Mobility Ratio

In test 1 where the mobility ratio at the back edge is 1.17, the FC tracer emerged at 0.859 PV after the injection of chase brine. The mixing-zone length was 1.06 ft. Comparison between test 1 and test 2 (FC emerged at 0.864 PV and the mixing-zone length was 1.14 ft) shows that both chase brine breakthrough and mixing-zone length are practically unchanged by the small change of mobility ratio from 1.17 to 1.56, although they show a slight increase with increasing mobility ratio.

Effect of Flow Rate

At a flow rate of 1.27 ft/day, tracer FC emerged at 0.81 PV in test 4 and 0.68 PV in test 5 after the injection of chase brine. The mixing-zone lengths were 1.76 ft in test 4 and 2.08 ft in test 5. This means that in the purely viscous flow regime, Pusher 500 gives more viscous fingering than does glycerin. Comparison between the tests with glycerin at both high and low flow rates (tests 3 and 4) shows that though the breakthrough of chase water is almost unchanged with flow rate, the mixing-zone length increases with flow rate. This indicates that viscous fingering increases with flow rate for Newtonian fluids. For Pusher 500, the effect of flow rate on viscous fingering is different. As shown in table 1, increasing the flow rate from 1.27 to 18.1 ft/day decreases the mixing-zone length from 2.08 to 1.14 ft. Chase water broke through sooner at 1.27 ft/day than at 18.1 ft/day. This means that for Pusher 500, viscous fingering decreases with flow rate. The decrease in viscous fingering at a high flow rate can be attributed to the viscoelasticity effect, since 18.1 ft/day is in the viscoelastic flow regime.

At the trailing edge, a denuded zone as indicated by the viscosity profile, exists between 4.07 and 4.4 PV in test 2 (Fig. 8). In this zone, both polymer and glycerin concentrations are low. The viscosities of the

effluents drop from 8.1 to 3.1 cp. This is caused by IPV and viscous fingering effects. In this region, the displacement of the trailing polymer is unstable. Similar results have also been observed in the other two tests with Pusher 500.

From 4.4 to 4.5 PV, the viscosity increases from 3.1 to 8.3 cp, indicating the existence of a favorable mobility ratio in this zone. This is due to the increase in glycerin concentration. Because of a favorable mobility ratio, the displacement in this zone is piston-like, and the spreading out of tracer concentration profiles is due to dispersion. Such a piston-like displacement zone does not exist at the trailing edge of the 63 wt pct glycerin solution. This could explain why Pusher 500 shows less viscous fingering than does glycerin solution. However, in the tests at a low flow rate (1.27 ft/day), where the flow is purely viscous, glycerin shows a more stable displacement than does Pusher 500 even though a piston-like displacement zone exists at the back edge of Pusher 500. Hence, that viscoelasticity tends to suppress viscous fingering is obvious. This also means that the slug size of the mobility buffer required in chemical flooding at reservoir conditions would be smaller for a Newtonian fluid than for a non-Newtonian fluid.

CONCLUSIONS

The main conclusions of this study are as follows:

1. At both high and low flow rates, a Newtonian fluid gives a more stable displacement at the front end than does the non-Newtonian fluid; the dispersion coefficient of tracer in Pusher 500 is higher than that in glycerin solution.
2. Dynamic stability increases with decreasing mobility ratio at both the leading and trailing edges. When the mobility ratio is favorable, the change in dispersion coefficient is proportional to the change in mobility ratio.

3. At the trailing edge where the mobility ratio is unfavorable, Pusher 500 gives less viscous fingering than does glycerin when the flow rate is in the viscoelastic flow regime. In the viscous flow regime, glycerin has less viscous fingering than does Pusher 500. Viscoelasticity tends to suppress viscous fingering. For Newtonian fluids, increasing the flow rate increases viscous fingering.
4. The slug size of the mobility buffer required in chemical flooding at reservoir conditions would be less for a Newtonian fluid than for a non-Newtonian fluid.

REFERENCES

1. Dawson, R. and R. B. Lantz. Inaccessible Pore Volume in Polymer Flooding. SPEJ, October 1972, pp. 448-452.
2. Gupta, S. P. and S. P. Trushenski. Micellar Flooding - The Propagation of the Polymer Mobility Buffer Bank. SPEJ, February 1978, pp. 5-12.
3. Shah, B. N., G. P. Willhite, and D. W. Green. The Effect of Inaccessible Pore Volume on the Flow of Polymer and Solvent Through Porous Media. Pres. at the 53rd Annual Tech. Conf. of SPE of AIME, Houston, Oct. 1-3, 1978. SPE paper 7586.
4. Patton, J. T., K. H. Coats, and G. T. Colegrove. Prediction of Polymer Flood Performance. SPEJ, March 1971, pp. 72-84.
5. Lecourtier, J. and G. Chauveteau. Propagation of Polymer Slugs Through Porous Media. Pres. at the 59th SPE Annual Tech. Conf., Houston, Sept. 16-19, 1984. SPE paper 13034.
6. Dietzel, H. J. and G. Pusch. Laboratory Investigations on the Dynamic Stability of Polymer Slugs. Pres. at the SPE Sixth Intl. Symp. on Oilfield and Geothermal Chemistry, Dallas, Jan. 25-27, 1982. SPE paper 10614.
7. Sorbie, K. S., A. Parker, and P. J. Clifford. Experimental and Theoretical Study of Polymer Flow in Porous Media. Pres. at the 60th Annual Conf. of the SPE, Las Vegas, Sept. 22-25, 1985. SPE paper 14231.
8. Mast, M. E. Longitudinal Mixing Characteristics of Miscible Polymer Displacement Experiments in Porous Media. M. S. Thesis, Univ. of Kansas, 1979.

9. Vossoughi, S., J. E. Smith, D. W. Green, and G. P. Willhite. A New Method to Simulate the Effects of Viscous Fingering on Miscible Displacement Processes in Porous Media. SPEJ, Feb. 1984, pp. 56-64.
10. Smith, F. W. The Behavior of Partially Hydrolyzed Polyacrylamide Solutions in Porous media. J. Pet Tech., February 1970, pp. 148-156.
11. Stanislav, J. F. and C. S. Kabir. Polymer Flow Behavior as Applied to Enhanced Recovery. J. Canadian Pet. Tech., April-June, 1977, Montreal, pp. 91-97.
12. Friedmann, F. Surfactant and Polymer Losses During Flow Through Porous Media. Pres. at the Intl. Symp. on Oilfield and Geothermal Chemistry, Denver, June 1-3, 1983. SPE paper 11779.
13. Omar, A. E. Effect of Polymer Adsorption on Mobility Control. Pres. at the SPE Middle East Oil Technical Conference, Manama, Bahrain, Mar. 14-17, 1983. SPE paper 11503.
14. Omar, A. E. Plugging and Adsorption Problems with Tertiary Polymers. Oil and Gas J., Nov. 8, 1982, pp. 193-197.
15. Lakatos, I. and J. Lakatos-Szabq. Investigation of the Sorption Phenomena of Polyacrylamides in Porous Media Under Dynamic Conditions, I: Effect of the Polymer Type and Concentration, and Foreign Electrolytes on the Amount of Adsorbed Polymer. Acta Chim. Acad. Sci. Hung., 1980, v. 105, No. 1, pp. 57-72.
16. Klein, J. and A. Westerkamp. Comparative Adsorption Studies Using a Polyacrylamide and a Polysaccharide Type Polymer in Oilfield Oriented Model Systems Simulating Enhanced Oil Recovery Conditions. Die Angewandte Makromolekulare Chemie (1980), No. 92, pp. 15-31.
17. Duda, J. L., E. E. Klaus, and S. K. Fan. Influence of Polymer-Molecule/Wall Interactions on Mobility Control. SPEJ., October 1981, pp. 613-622.
18. Meister, J. J., H. Pledger, Jr., T. E. Hogen-Esch, and G. B. Butler. Retention of Polyacrylamide by Berea Sandstone, Baker Dolomite, and Sodium Kaolinite During Polymer Flooding. Pres. at the SPE 5th Intl. Symp. on Oilfield and Geothermal Chemistry, Stanford, May 28-30, 1980. SPE paper 8981.
19. Klein, J. and W. M. Kulicke. Polymer-Polymer and Polymer-Solid Interaction and Their Relevance for Polymer Application in Enhanced Oil Recovery. Pres. at the SPE 5th Intl. Symp. on Oilfield and Geothermal Chemistry, Stanford, May 28-30, 1980. SPE paper 8980.

20. Mungan, N. Rheology and Adsorption of Aqueous Polymer Solutions. *J. of Canadian Pet.*, April-June 1969, pp. 45-50.
21. Baijal, S. K. and N. C. Dey. Role of Molecular Parameters During Flow of Polymer Solutions in Unconsolidated Porous Media. *J. Applied Polym. Sci.*, 1982, v. 27, pp. 121-131.
22. Szabo, M. T. Some Aspects of Polymer Retention in Porous Media Using a C-14-Tagged Hydrolyzed Polyacrylamide. *SPE J.*, August 1975, pp. 323-337.
23. Gogarty, W. B. Mobility Control with Polymer Solutions. *SPEJ.*, June 1967, pp. 161-170.
24. Harrington, R. E. and B. H. Zimm. Anomalous Plugging of Sintered Glass Filters by High Molecular Weight Polymers. *J. Polym. Sci., Part A-2*, v. 6, 1968, pp. 294-299.
25. Dominguez, J. G. and G. P. Willhite. Retention and Flow Characteristics of Polymer Solutions in Porous Media. *SPEJ.*, April 1977, pp. 111-121.
26. Huff, R. V. Dependence of Polymer Retention on Flow Rate. *J. Pet. Tech.*, November 1973, pp. 1307-1308.
27. Chauveteau, G. Molecular Interpretation of Several Different Properties of Flow of Coiled Polymer Solutions Through Porous Media in Oil Recovery Conditions. Pres. at the 56th SPE Ann. Fall Tech. Conf., San Antonio, Oct. 5-7, 1981. SPE paper 10060.
28. Willhite, G. P. and J. G. Dominguez. Mechanisms of Polymer Retention in Porous Media. In *Improved Oil Recovery by Surfactant and Polymer Flooding*, D. O. Shah and R. S. Schechter, eds., Academic Press, Inc., New York, 1977, p. 511.
29. Liauh, W. C., J. L. Duda, and E. E. Klaus. An Investigation of the Inaccessible Pore Volume Phenomena. *Interfacial Phenomena in Enhanced Oil Recovery*, AIChE Symp. Series, 1982, v. 78, No. 212, pp. 70-76.
30. Perkins, T. K. and O. C. Johnston. A Review of Diffusion and Dispersion in Porous Media. *SPEJ*, March 1963, pp. 70-84.
31. Brigham, W. E., P. W. Reed, and J. N. Dew. Experiments on Mixing During Miscible Displacement, *SPEJ*, March 1961, pp. 1-8.
32. Perrine, R. L. The Development of Stability Theory for Miscible Liquid-Liquid Displacement. *SPEJ*, March 1961, pp. 17-25.
33. Giordano, R. M., S. J. Salter, and K. K. Mohanty. The Effect of Permeability Variation on Flow in Porous Media. Pres. at the 60th Ann. Conf. of SPE, Las Vegas, Sept. 22-25, 1985. SPE paper 14365.

34. Gao, H. W., P. B. Lorenz, and S. Brock. Viscoelastic Behavior of Hydrolyzed Polyacrylamide Solutions in Porous Media. Poly. Mater. Sci. Eng., Proc. of the ACS Div. of Polymeric Materials: Sci. and Eng., v. 55, Fall Mtg., Anaheim, CA, 1986, pp. 685-693.
35. Gao, H. W., P. B. Lorenz, and S. Brock. Rheological Behavior of Pusher 500 Under a Variety of Chemical and Thermal Conditions. Dept. of Energy Report No. NIPER-225, Nov. 1986, 43 pp.
36. Jennings, R. R., J. H. Rogers, and T. J. West. Factors Influencing Mobility Control by Polymer Solutions. J. Pet. Tech., March 1971, pp. 391-401.
37. Scoggins, M. W. and J. W. Miller. Spectrophotometric Determination of Water-Soluble Organic Amides. Anal. Chem., v. 47, 1975, pp. 152-154.
38. Chauveteau, G. Rodlike Polymer Solution Flow Through Fine Pores: Influence of Pore Size on Rheological Behavior. J. Rheol., v. 26, No. 2, 1982, pp. 111-142.
39. Blackwell, R. J., J. R. Rayne, and W. M. Terry. Factors Influencing the Efficiency of Miscible Displacement. Trans., AIME, v. 216, 1959, pp. 1-8.